The Journal of Immunology

Exacerbation of Experimental Autoimmune Encephalomyelitis in P2X $_7$R$^{-/-}$ Mice: Evidence for Loss of Apoptotic Activity in Lymphocytes

Lanfen Chen and Celia F. Brosnan

J Immunol 2006; 176:3115-3126; ;
doi: 10.4049/jimmunol.176.5.3115
http://www.jimmunol.org/content/176/5/3115

The Journal of Immunology is published twice each month by
The American Association of Immunologists, Inc.,
1451 Rockville Pike, Suite 650, Rockville, MD 20852

Print ISSN: 0022-1767 Online ISSN: 1550-6606.

Exacerbation of Experimental Autoimmune Encephalomyelitis in $P2X_7R^{-/-}$ Mice: Evidence for Loss of Apoptotic Activity in Lymphocytes[1]

Lanfen Chen[2] and Celia F. Brosnan

The purinergic receptor $P2X_7R$ is a nucleotide-gated ion channel that has been proposed to function as a major regulator of inflammation. In this study we examined the role of this receptor in regulating inflammation in the CNS by determining the effects of the loss of this receptor ($P2X_7R^{-/-}$) on experimental autoimmune encephalomyelitis (EAE), an animal model for multiple sclerosis. We show here that $P2X_7R^{-/-}$ mice developed more severe clinical and pathological expression of EAE than wild type (WT) controls and that spleen and lymph node cells from $P2X_7R^{-/-}$ mice proliferated more vigorously to Ag in vitro. Bone marrow (BM) radiation chimeras revealed that enhanced susceptibility to EAE was detected in chimeric mice of WT host engrafted with $P2X_7R^{-/-}$ BM cells, indicating that the genotype of the BM cells regulated disease susceptibility. Coculture of $P2X_7R^{-/-}$ macrophages with WT lymphocytes and vice versa showed that enhanced proliferative activity resided within the $P2X_7R^{-/-}$ lymphocyte population and correlated with reduced levels of IFN-γ and NO and apoptosis of lymphocytes. mRNA and protein for IFN-γ were also significantly reduced in the CNS of $P2X_7R^{-/-}$ mice with EAE. FACS analysis of cells isolated from the CNS showed significantly fewer annexin V/propidium iodide-positive lymphocytes in the CNS of $P2X_7R^{-/-}$ mice early in the disease, and TUNEL staining of inflamed CNS tissues supported this result. From these data we conclude that enhanced susceptibility of $P2X_7R^{-/-}$ mice to EAE reflects a loss of apoptotic activity in lymphocytes, supporting an important role for this receptor in lymphocyte homeostasis. *The Journal of Immunology,* **2006, 176: 3115–3126.**

The $P2X_7$ receptor, $P2X_7R$, is a member of the ionotropic family of purinergic receptors that respond to extracellular nucleotides and nucleosides (1–3). It differs from other members of this family, however, in its relatively low affinity for ATP, the presence of a long C-terminal region that contains several protein-protein interaction domains, and the activation of two membrane conductance states upon receptor ligation. Following brief exposure to ATP a nonselective cation channel is activated, whereas following prolonged or repeated applications of high dose ATP multimeric channels or pores may form that allow passage of solutes as large as 900 kDa (1–5).

Although widely expressed in many cell types, the $P2X_7R$ has generated much interest in cells of the immune system due to its role in the ATP-dependent processing and release of proinflammatory mediators such as IL-1 and TNF (6–9). It has also been implicated in the activation and maturation of T cells (10, 11), the formation of giant cells (12, 13), the killing of invading microorganisms in macrophages (14–16), the activation of the inducible form of NO synthase (17, 18), and the shedding of L-selectin (CD62L) (19, 20), an adhesion molecule that functions in leukocyte binding to the activated endothelium and in lymphocyte homing to high endothelial venules.

The involvement of the $P2X_7R$ in regulating factors involved in inflammation has suggested that the loss of function of this receptor might lead to the amelioration of diseases of an inflammatory nature. Consistent with this possibility are the observations in mice in which the gene for the $P2X_7R$ has been inactivated ($P2X_7R^{-/-}$) (21, 22). As expected, peritoneal macrophages isolated from these animals failed to release bioactive IL-1β following LPS activation and stimulation with ATP (21, 22). However, perhaps of even greater interest was the observation that in vivo the inflammatory response was attenuated in mice made arthritic using anti-collagen Abs and challenge with LPS, with both the incidence and severity of disease being significantly reduced in $P2X_7R^{-/-}$ mice (20). Similarly, in two models of chronic pain, one neuropathic and the other inflammatory in origin, inactivation of the $P2X_7R$ resulted in significant amelioration of hypersensitivity to both mechanical and thermal stimuli, which, in the chronic inflammatory pain model, correlated with reduced protein, but not reduced mRNA, for IL-1 (22).

The $P2X_7R$ may also play an important role in regulating inflammatory and immune responses through its cytolytic activity. In several cell types, the channel-to-pore transition is associated with loss of membrane potential and permeabilization of the cell membrane, leading ultimately to cell death (23–25). This ATP-dependent cytotoxicity has been best studied in macrophages, where it has been found that cell death can occur via either a necrotic or an apoptotic process. The picture is more complex in lymphocytes. In B cells, permeability assays indicate the formation of a much smaller pore following activation with ATP than that found in macrophages, and B cells show only a low level of susceptibility to ATP-mediated cytotoxicity (26, 27). In T cells, it has been proposed that cell lysis occurs through a mechanism involving NAD-dependent ribosylation by ADP-ribosyltransferase (ART)[3] 2.

Department of Pathology, Albert Einstein College of Medicine, Bronx, NY 10461

Received for publication June 7, 2005. Accepted for publication December 23, 2005.

The costs of publication of this article were defrayed in part by the payment of page charges. This article must therefore be hereby marked *advertisement* in accordance with 18 U.S.C. Section 1734 solely to indicate this fact.

[1] This work was supported by National Institute of Neurological Disorders and Stroke, National Institutes of Health, U.S. Public Health Service Grants NS40137 and NS11920.

[2] Address correspondence and reprint requests to Dr. Lanfen Chen, Department of Pathology, Albert Einstein College of Medicine, 1300 Morris Park Avenue, Bronx, NY 10461. E-mail address: lachen@aecom.yu.edu

[3] Abbreviations used in this paper: ART, ADP-ribosyltransferase; adh, adherent; BM, bone marrow; CLL, chronic lymphocytic leukemia; DAPI, 4′,6′-diamidino-2-phenylindole; DC, dendritic cell; EAE, experimental autoimmune encephalomyelitis; KO, knockout; MOG, myelin oligodendrocyte glycoprotein; PF, paraformaldehyde; PI, propidium iodide; sus, nonadherent; WT, wild type.

0022-1767/06/$02.00

ART2 is a toxin-related ectoenzyme that is expressed by T cells, and the exposure of mature T cells to NAD induces cell death. Recent studies have shown that ART2-catalyzed ADP ribosylation activates $P2X_7R$, resulting in calcium flux, shedding of CD62L, cell shrinkage, phosphatidylserine exposure, and propidium iodide (PI) uptake (28, 29). These findings demonstrate that the key mediator of NAD-induced cell death is the $P2X_7R$, with activation occurring through much lower doses of NAD than what is found with ATP. Of particular interest to the regulation of immune-mediated diseases are the very recent studies that have shown that $CD4^+CD25^+$ T regulatory cells are particularly sensitive to this mechanism of cell death, resulting in increased levels of $CD4^+CD25^+$ regulatory T cell activity in $P2X_7R^{-/-}$ mice (30).

In this study, we have explored a role for the $P2X_7R$ in the generation of an autoimmune response by investigating the susceptibility of $P2X_7R^{-/-}$ mice to experimental autoimmune encephalomyelitis (EAE). EAE is an inflammatory demyelinating disease of the CNS that functions as the principal animal model for multiple sclerosis (31). It can be induced in susceptible species by active or adoptive sensitization to myelin Ags, and passive transfer experiments initially implicated a $CD4^+$ T cell population that expressed a Th1-type cytokine profile as effector T cells (31, 32). However, more recently a newly identified Th cell subset that expresses IL-17 (Th17) has been implicated, with both IFN-γ and IL-4 acting as regulatory cytokines (33–35). Activated macrophages, as well as macrophage-derived cytokines such as IL-1 and TNF, have also been shown to participate in disease pathogenesis (36, 37). Depending upon the species used and age at the time of sensitization, as well as the specific myelin Ag chosen, EAE may present as an acute monophasic episode of paralysis or may develop into a more chronic syndrome that shows periods of remission and exacerbation (reviewed in Ref. 31). Lesions within the CNS are most prevalent in the white matter tracts of the lumbar region of the spinal cord and are characterized by edema and perivascular infiltrates of inflammatory cells (32). The extent of myelin loss and axonal degeneration usually reflects the severity of the inflammatory response (32). Using the myelin oligodendrocyte glycoprotein (MOG)-induced model of EAE in the C57BL/6 mouse, we show herein that mice deficient in $P2X_7R$ function are more susceptible to EAE than wild type (WT) mice and show enhanced inflammation in the CNS.

Materials and Methods

Animals and reagents

$P2X_7R^{-/-}$ mice back-crossed for 12 generations to C57BL/6 mice were supplied by Dr. C. A. Gabel (Pfizer) (21) and bred at the Albert Einstein College of Medicine (Bronx, NY). WT C57BL/6 mice were obtained from the same source (C57BL/6Ntac; Taconic Farms). Successful truncation of the $P2X_7R$ was confirmed by PCR (primer sequences used were as follows: WT, 5′-GCA GCC CAG CCC TGA TAC AGA CAT T-3′ and 5′-TCG GGA CAG CAC GAG CTT ATG GA-3′; knockout (KO), 5′-GAC AGC CCG AGT TGG TGC CAG TGT G-3′ and 5′-GGT GGG GGT GGG GGT GGG ATT AGA T-3′) (38). All animals were housed and maintained in a federally approved animal facility, and the Animal Care and Use Committee of Albert Einstein College of Medicine approved all protocols.

Induction of EAE

EAE was induced in mice (at 7–9 wk) by s.c. immunization with 300 μg of MOG_{35-55} peptide (MEVGWYRSPFSRVVHLYRNGK; Celtek Bioscience) in a 200-μl emulsion of IFA containing 300 μg/ml *Mycobacterium tuberculosis* H37Ra (Difco) in the lower dorsum twice, 1 wk apart. The mice received i.p. 500 ng of pertussis toxin (Sigma-Aldrich) on the first day of sensitization and 2 days later. The day after the last injection of MOG was considered day 1. EAE was scored as follows: 0, no symptoms; 1, floppy tail; 2, hind limb weakness; 3, hind limb paralysis; 4, forelimb and hind limb paralysis; and 5, death. In experiments that investigated the role of peripheral mononuclear cells in disease expression, splenocytes (20×10^6) from naive WT mice were injected i.p. into $P2X_7R^{-/-}$ mice after lysis of RBCs and extensive washing 6 days before sensitization with MOG.

Bone marrow (BM) chimeras

BM cells were harvested from the long bones of C57BL/6 or $P2X_7R^{-/-}$ mice by flushing with cold PBS. RBCs were removed using RBC lysis buffer (Sigma-Aldrich). Cells were deaggregated by gently cycling through a 26-gauge needle and then through a 70-μm BD Falcon nylon cell strainer (BD Discovery Labware). Cells were washed three times, counted, and transferred i.v. at 6×10^6 cells/recipient. Recipients (3- to 4-wk-old mice) were prepared by one dose of whole body irradiation with 700 rads from a cesium-137 source. BM cells were transferred within 5 h after irradiation. Blood samples were checked for successful engraftment using PCR. Mice were maintained in quarantine for 5–6 wk before EAE sensitization.

Histological analysis

For pathologic analysis of the tissue, EAE mice were anesthetized at indicated times and perfused by intracardiac infusion of 4% paraformaldehyde (PF) in PBS or Trump's solution (4% PF and 1% glutaraldehyde in 0.1 M phosphate buffer (pH 7.4)). The paraffin sections were prepared from 4% PF-fixed tissues and representative sections stained with H&E. The tissues fixed in Trump's solution were dehydrated and embedded in Epon, and sections were stained with toluidine blue as described previously (39). An inflammatory index was determined by counting the number of lesions per section and multiplying by a factor of 1–5, representing the intensity of the inflammatory infiltrate.

Isolation of CNS infiltrating mononuclear cells

The isolation of CNS mononuclear cells using Percoll gradients was as described previously (39). Mononuclear cells were collected from the 37:70% Percoll interface, washed in medium containing 10% FCS, and counted.

Proliferation assay

Spleen and lymph node cells were isolated by passage through a stainless steel mesh grid in sterilized RPMI 1640. RBCs were lysed with RBC lysis buffer (Sigma-Aldrich), washed twice in 10% FCS/RPMI 1640, and counted. Cells were resuspended in complete RPMI 1640 medium containing 10% FCS, 1% penicillin and streptomycin, 2 mM glutamine, 1 mM sodium pyruvate, 20 mM HEPES (all from Invitrogen Life Technologies), and 1% nonessential amino acids (Sigma-Aldrich) at a density of 2×10^6 cells/ml, plated in 96-well plates (200 μl per well), and cultured without or with indicated concentrations of the Ag MOG_{35-55}. At day 5, proliferation assays were performed using a cell proliferation ELISA BrdU (colorimetric) kit as per the instruction manual (Roche).

Spleen cell mix and match experiment

The single-cell suspension from spleen was prepared as described in the previous paragraph. Cultured spleen cells were incubated in 96-well tissue culture plates at 37°C for 2 h in a CO_2 incubator to separate adherent cells and cells in suspension. Suspension cells in medium were transferred to another plate, and the adherent cells remaining in the original plate were washed once using warmed fresh medium. After washing, the cells in suspension were transferred to the plates containing adherent cells. The mixture of suspension cells and adherent cells were cultured with or without the indicated concentrations of the Ag MOG_{35-55}.

Dendritic cells (DCs) were prepared from adult BM of WT or $P2X_7R^{-/-}$ mice. Briefly, BM cells were harvested from the long bones by insufflation and plated on 24-well plates at a cell density of 2.0×10^6/ml in complete DMEM with 10% FCS containing 10 ng/ml mouse recombinant GM-CSF (R&D Systems). Cells were fed every 2 days with complete DMEM containing 10 ng/ml GM-CSF. Cells were harvested after 6 days, and the surface phenotype was confirmed by FACS analysis for the expression of cell surface CD11c, MHC II, CD80 (B7.1), and CD86 (B7.2) (BD Pharmingen). CD4 cells were purified from spleens of MOG-sensitized mice using a $CD4^+$ T cell isolation kit (Milteny Biotec). Cells were plated in 96-well plates at a density of 4×10^5 $CD4^+$ T cells and 1×10^5 DCs in the combinations WT_{dc} plus WT_{cd4}, WT_{dc} plus KO_{cd4}, KO_{dc} plus KO_{cd4}, and KO_{dc} plus WT_{cd4}. The cells were stimulated with MOG as described above for 3 days.

TUNEL staining

Apoptosis was detected on paraffin sections or cultured cells by an ApopTag peroxidase in situ apoptosis detection kit (Chemicon International)

according to the manufacturer's instructions. Digital images were collected using an Olympus digital camera and processed using Adobe Photoshop 7.0.1. (Adobe Systems).

Immunohistochemistry

Paraffin-embedded sections were deparaffinized and boiled for Ag retrieval in sodium citrate buffer (DakoCytomation) for 20 min. Sections were then incubated with 3% H_2O_2 for 30 min and blocked in 10% normal goat serum for 1 h at room temperature. Tissues were stained for 2 h at room temperature with the anti-CD3ϵ Ab (145-2C11; BD Pharmingen) at 1/100 dilution in 5% normal goat serum/PBS. After washing twice in PBS, Cy2-conjugated goat anti-Armenian hamster IgG at 1/200 (Jackson ImmunoResearch Laboratories) was applied for 2 h at room temperature, counterstained for 15 min at room temperature with 1 μg/ml 4′,6′-diamidino-2-phenylindole (DAPI) dihydrochloride hydrate/PBS solution, and mounted in aqueous mounting medium (Gel/Mount; Biomeda). Fluorescence microscopy was performed on an Olympus IX70 with ×60 numerical aperture and 1.4 infinity-corrected optics. Images were collected with a Photometrics cooled charge-coupled device camera with a KAF 1400 chip using IPLab Spectrum (Scanalytics).

Flow cytometry assay

For annexin V-PI staining, cells were incubated with Annexin V^{FITC} (BD Pharmingen) and PI (Sigma-Aldrich) in 100 μl of 1× annexin V binding buffer at room temperature for 15 min. An additional 400 μl of 1× annexin V binding buffer was then added, and cells were analyzed using CellQuest software in a FACScan cytometer (BD Biosciences).

For ART2.2 and CD3 staining, cells were blocked with purified rat anti-mouse CD16/CD32 (Fcγ III/II receptor) mAb in FACS staining buffer (1× PBS containing 1% BSA and 0.05% NaN_3) for 20 min on ice. The cells were then incubated with PE-conjugated rat anti-mouse CD3 mAb (IgG_{2b}, 17A2; BD Pharmingen) and purified rat anti-mouse ART2.2 mAb (IgG_{2a}, Nika102; BD Pharmingen) for 20 min on ice, washed twice with FACS staining buffer, and further incubated with FITC-conjugated mouse anti-rat IgG_{2a} mAb for 20 min on ice. Cells were washed twice in PBS, fixed in 400 μl of 1% PF, and analyzed using CellQuest software in a FACScan cytometer. Postacquisition analysis was performed using FCS Express software (De Novo Software).

Cytokine assay

The protein level of Th1/Th2 cytokines was quantified using FAST Quant mouse Th1/Th2 kit (Whatman Schleicher & Schuell) according to the manufacturer's instructions. The IFN-γ levels in cell culture supernatants were also quantified using Quantikine ELISA kit (R&D Systems). EAE animals were perfused with cold PBS, and the spinal cord was removed, snap-frozen in dry ice, and stored at −80°C. Spinal cord samples were sonicated in PBS containing protease and phosphatase inhibitors and centrifuged at 14,000 rpm for 30 min, and the supernatant was taken for assay. For cell culture supernatants, samples were centrifuged at 14,000 rpm for 20 min.

Real-time quantitative PCR

Spinal cord samples were homogenized in TRIzol reagent (Invitrogen Life Technologies). RNA was extracted according to the manufacturer's instructions, and genomic DNA was removed with DNase I. Quantitative PCR was performed as described previously using SYBR Green quantitative PCR master mix (Applied Biosystems) (40). All runs were accompanied by two internal control genes, β-actin and GAPDH. Samples were normalized using a $\Delta\Delta$ cycle threshold-based algorithm to give arbitrary units representing relative expression levels between samples. The following primers were used: IL-1β, 5′-CAG GCA GGC AGT ATC ACT CA-3′ (forward) and 5′-TGT CCT CAT CCT GGA AGG TC-3′ (reverse); IL-6, 5′-CCG GAG AGG AGA CTT CAC AG-3′ (forward) and 5′-TCC ACG ATT TCC CAG AGA AC-3′ (reverse); IFN-γ, 5′-ACT GGC AAA AGG ATG GTG AC-3′ (forward) and 5′-GCT GAT GGC CTG ATT GTC TT-3′ (reverse); TNF-α, 5′-ACG GCA TGG ATC TCA AAG AC-3′ (forward) and 5′-GTG GGT GAG GAG CAC GTA GT-3′ (reverse); β-actin, 5′-TAC CAC AGG CAT TGT GAT GG-3′ (forward) and 5′-TTT GAT GTC ACG CAC GAT TT-3′ (reverse); and GAPDH, 5′-AAC TTT GGC ATT GTG GAA GG-3′ (forward) and 5′-ACA CAT TGG GGG TAG GAA CA-3′ (reverse).

Measurement of NO production

The amount of accumulated nitrite (NO) in cell-free supernatants was determined by the calorimetric Griess reaction, as described previously (41).

Statistics

Statistical analysis was performed using Prism software. Statistical significance of all results was assessed using Student's *t* test or a Mann-Whitney *U* test. A *p* value of <0.05 was considered significant.

Results

$P2X_7R^{-/-}$ mice show enhanced susceptibility to EAE compared with WT mice

To define the role of the $P2X_7R$ in the regulation of CNS inflammation and demyelination, gender- and age-matched $P2X_7R^{-/-}$ and WT C57BL/6 mice were sensitized to develop EAE by active immunization with the $MOG_{35–55}$ peptide and examined on a daily basis for the clinical expression of disease. Contrary to our expectations given its known role in regulating inflammation, the $P2X_7R^{-/-}$ mice developed a more severe form of EAE characterized by higher clinical scores during both the acute and chronic stages of the disease when compared with matched WT mice (Fig. 1). The differences between $P2X_7R^{-/-}$ mice and WT mice were statistically significant for both males and females but were particularly evident in females due to the less severe disease in WT mice. However, no difference in the clinical index was noticed between the male and female $P2X_7R^{-/-}$ mice. In addition, no differences were noted between WT and $P2X_7R^{-/-}$ mice regarding the day of onset, time of peak expression of disease, or incidence (Table I).

$P2X_7R^{-/-}$ mice show more severe pathology in the CNS

In both WT and $P2X_7R^{-/-}$ mice, white matter lesions typical of acute EAE were observed in the spinal cord (Fig. 2, *A–D*). These lesions consisted of perivascular inflammatory infiltrates of mononuclear and polynuclear cells and evidence of demyelination and axonal degeneration (Fig. 2, *C* and *D*). To determine whether the cellular profile of these inflammatory infiltrates differed between WT and $P2X_7R^{-/-}$ mice, we performed a FACS analysis of cells isolated from the spinal cord. Spleen and lymph node cells were examined in parallel. No differences were noted for any of these cell types in spleen and lymph node preparations. Similarly, in the CNS cellular infiltrates no differences were noted in the percentage representation for $CD4^+$, $CD8^+$, $B220^+$, and $Gr1^+$ cells between the two groups of mice. However, statistically significant increases in the percentage of $CD45^{high}CD11b^+$ macrophages were detected in infiltrates from the spinal cord of $P2X_7R^{-/-}$ mice (Table II).

Analysis of lesion distribution showed that in the $P2X_7R^{-/-}$ mice the lesions were more extensive than those present in WT mice (see areas marked in red in Fig. 2, *A* and *B*). The most striking difference between WT and $P2X_7R^{-/-}$ mice was the more extensive involvement of the brain and cerebellum in $P2X_7R^{-/-}$ mice, areas of the CNS not typically involved to any great extent in EAE (Fig. 2, *F–K*). As shown in Fig. 2*G* (arrows) and at higher power in Fig. 2*I*, the brain and cerebellum showed numerous small perivascular lesions predominantly associated with white matter tracts. These lesions were much less frequent in the WT mice (Fig. 2*F*), and similar small vessels were not usually inflamed in WT brains (Fig. 2*H*). An increase in lesion frequency was also detected in the cerebellum (Fig. 2, compare *K* with *J*). Quantification of lesions in these tissues showed a significant increase in their number in $P2X_7R^{-/-}$ mice (Fig. 2*L*).

Spleen cell transfer partially reverses disease exacerbation in $P2X_7R^{-/-}$ mice

The $P2X_7R$ is known to be widely expressed in both the peripheral immune system as well as in cells endogenous to the CNS (5, 42). As a first step in exploring whether loss of $P2X_7R$ function that resulted in disease exacerbation was due to its role in cells of the

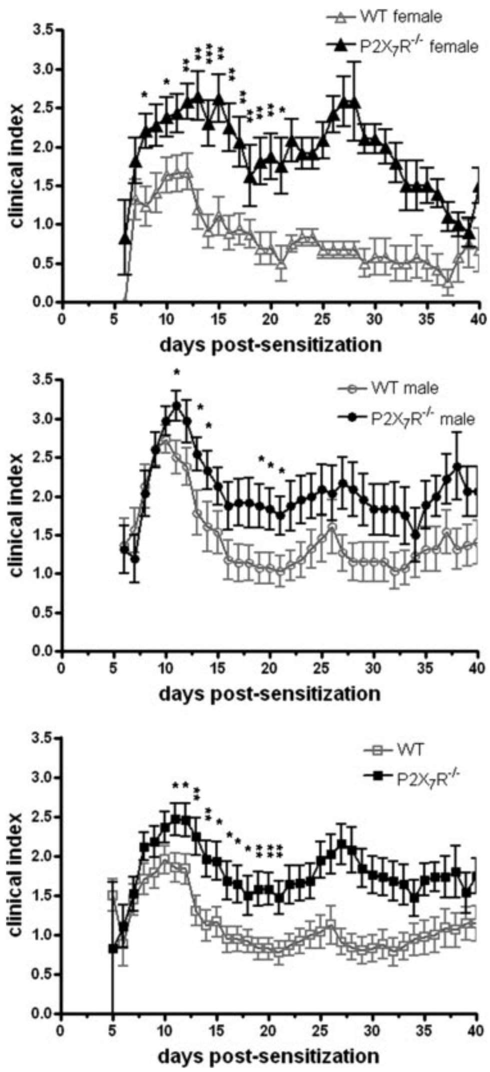

FIGURE 1. $P2X_7R^{-/-}$ mice develop more severe EAE than do WT C57BL/6 mice. Mice were sensitized to develop EAE using MOG_{35-55} and evaluated for clinical expression of disease as described in *Materials and Methods*. Data are derived from at least four independent experiments for each gender and are expressed as mean ± SEM ($n \geq 9$ per group and per experiment). The *p* values refer to comparisons between $P2X_7R^{-/-}$ and WT mice. *, $p < 0.05$, **, $p < 0.01$; ***, $p < 0.001$. *Top panel*, females; *middle panel*, males; *bottom panel*, combined data for females and males.

immune system or cells in the CNS, we transferred spleen cells between WT and $P2X_7R^{-/-}$ mice and sensitized these mice for EAE. As shown in Fig. 3*A*, $P2X_7R^{-/-}$ mice receiving WT spleen cells showed an acute disease course that closely resembled that found in WT mice who had been transferred with WT spleen cells. However, during the chronic phase of the disease these mice showed clinical scores that fell between those noted in the WT and $P2X_7R^{-/-}$ mice. These data suggest that, during the acute phase of the disease, increased susceptibility to EAE likely reflects a role for this receptor in the response of immune cells to sensitization.

Radiation of BM chimeras confirmed a role for $P2X_7R^{-/-}$ leukocytes in disease exacerbation

To establish further the critical role of the $P2X_7R$ in the response of immune cells to Ag, we established BM chimeras. In these mice, enhanced susceptibility to EAE was noted in WT host animals receiving $P2X_7R^{-/-}$ BM cells when compared with WT host animals receiving WT BM cells (Fig. 3*B*). Similarly, EAE was

Table I. *Development of EAE induced in C57BL/6 WT and $P2X_7R^{-/-}$ mice*

EAE mice	Day of Onset[a]	Peak of Clinical Disease[a]	Incidence of Disease (%)
WT male	6.3 ± 0.6	9.0 ± 1.0	95.3 ± 8.1
$P2X_7$ KO male	6.3 ± 0.6	10.5 ± 0.5	100 ± 0.0
WT female	7.8 ± 1.4	12.0 ± 2.6	78.0 ± 19.1
$P2X_7$ KO female	6.8 ± 0.3	11.8 ± 2.8	83.3 ± 16.5

[a] The day after the last injection of MOG was considered day 1.

more severe in $P2X_7R^{-/-}$ animals receiving $P2X_7R^{-/-}$ BM cells compared with $P2X_7R^{-/-}$ host animals receiving WT BM cells (Fig. 3*C*). These data confirmed the important role of BM-derived cells in defining the enhanced susceptibility of $P2X_7R^{-/-}$ mice to EAE.

Analysis of spleen cell response to MOG peptide

To further investigate a role for the $P2X_7R$ in spleen cell responses to the MOG peptide, a proliferation assay was performed using cells isolated from animals that had been sensitized 7 days previously. The data showed that both spleen and lymph node cells isolated from $P2X_7R^{-/-}$ mice proliferated more vigorously to the MOG peptide than did cells isolated from WT mice (Fig. 4*A*). The $P2X_7R$ is known to regulate proinflammatory cytokine levels and cell death in both lymphocytes and macrophages (6–9, 14, 16). To test for possible differences in cytotoxic responses between WT and $P2X_7R^{-/-}$ mice, the extent of apoptosis present in these cultures was determined using TUNEL staining. TUNEL-positive cells were numerous in WT and $P2X_7R^{-/-}$ cultures incubated without Ag. However, in cultures stimulated with MOG, fewer lymphocytes were TUNEL-positive in spleen cells derived from $P2X_7R^{-/-}$ mice compared with those from WT mice (Fig. 4*B*). To determine whether this effect was due to the absence of a cytotoxic factor such as TNF from macrophages or to the loss of a cytotoxic response in lymphocytes, we transferred nonadherent (sus) spleen cells from WT mice (WT-sus) onto adherent (adh) cells from $P2X_7R^{-/-}$ (KO-adh) mice and vice-versa (KO-sus and WT-adh); these cells were then cultured for 5 days with MOG peptide. Control cultures consisting of WT plus WT or $P2X_7R^{-/-}$ plus $P2X_7R^{-/-}$ were prepared in parallel. As shown in Fig. 4*D*, the difference in proliferation between WT and $P2X_7R^{-/-}$ mice was found to reside predominantly within the nonadherent cell population, with only a minor effect being contributed by the adherent cells. To provide a more quantitative analysis of this effect, the experiment was then repeated and data were calculated as the fold increase over controls. Cumulative data for three additional experiments using 20 μg/ml MOG peptide gave values of ×5.5 for WT-adh plus KO-sus, ×1.7 for KO-adh plus WT-sus, ×2.8 for WT-adh plus WT-sus, and × 7.1 for KO-adh plus KO-sus (WT-adh plus KO-sus vs KO-adh plus WT-sus; $p < 0.01$, $n = 7$).

To address the possible mechanism for the difference in proliferation and apoptotic activity between WT and $P2X_7R^{-/-}$ mice, we assayed culture supernatants for cytokines and NO production from the mixed cell transfer experiment shown in Fig. 4*D*. No significant differences in the levels of IL-2 or IL-10 were detected in these culture supernatants (Fig. 4*F*). However, for IL-6, IFN-γ, IL-13, and NO, levels were significantly lower for cultures containing $P2X_7R^{-/-}$ lymphocytes as compared with the supernatants from cultures containing WT lymphocytes. Furthermore, these data correlated with the enhanced proliferation of $P2X_7R^{-/-}$ cells to Ag (Fig. 4*D*). IFN-γ production was also found to be dramatically decreased in supernatants from the $P2X_7R^{-/-}$ spleen cells cultured with MOG (20 μg/ml) shown in Fig. 4*A* (see Fig. 4*C*).

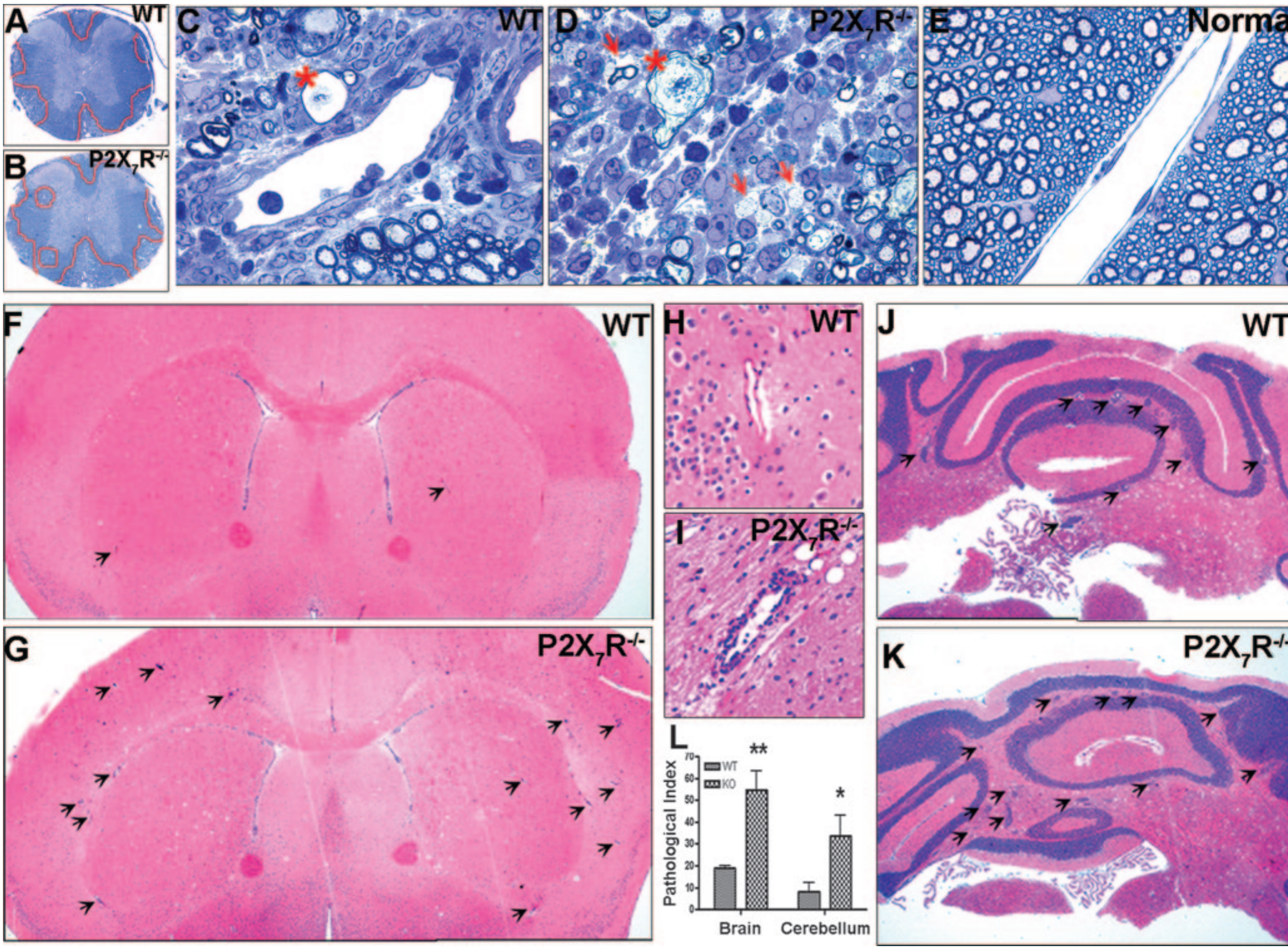

FIGURE 2. Pathological expression of EAE lesions in WT and $P2X_7R^{-/-}$ mice. *A* and *B*, One-micron toluidine blue-stained epoxy sections of the spinal cord show the submeningeal lesioned areas of the cord, which are outlined in red. Original magnification was ×10. *C* and *D*, Fine structure of the lesions within the anterior columns of the spinal cord shown in *A* and *B* are illustrated. Note the perivascular mononuclear and polymorphonuclear infiltrates, as well as evidence of axonal damage (asterisk) and demyelination (red arrows). *E*, Fine structure of a normal spinal cord. Original magnification was ×200. *F—K*, Paraffin embedded H&E stained sections of the brain (*F–I*) and cerebellum (*J* and *K*) at the peak of acute clinical disease (day 11). Arrows indicate the inflammatory lesions. In the brain, sites marked with arrows represent small perivascular lesions shown at higher power in *H*, and a typical vessel in WT is shown in *G*. Original magnification was ×5 for *F*, *G*, *J*, and *K* and ×80 for *H* and *I*. *L*, A pathological index representing lesion load was determined for the brain and cerebellum from $P2X_7R^{-/-}$ and WT mice ($n = 5$, per group) (in *L*, asterisk denotes values significantly different from the WT animals: $*$, $p < 0.05$; $**$, $p < 0.01$).

We then investigated whether differences in cytokine levels between WT and $P2X_7R^{-/-}$ mice could be detected in vivo during the acute phase of EAE. To test for these differences, we performed real-time PCR and protein array assays on spinal cord homogenates harvested on day 9. As shown in Table III, significantly reduced levels of mRNA and protein for IL-6 and IFN-γ were noted in $P2X_7R^{-/-}$ mice compared with WT mice, whereas no differences in protein for IL-2 and TNF-α were detected. Thus, the in vivo data support the result of the in vitro culture studies showing reduced IL-6 and IFN-γ in $P2X_7R^{-/-}$ mice with EAE. The data also show that, in agreement with the known role for the $P2X_7R$ in the processing and release of IL-1 (7), protein but not

Table II. *Cellular composition of leukocytes in WT and $P2X_7R^{-/-}$ mice*[a]

	$CD4^+$	$CD8^+$	$B220^+$	$CD45^+CD11b^+$	Gr-1^+
Spinal cord					
WT	34.3 ± 2.6	9.7 ± 0.7	9.1 ± 1.8	20.8 ± 1.3	22.1 ± 5.5
$P2X_7R^{-/-}$	28.3 ± 1.7	9.3 ± 1.9	11.3 ± 2.2	26.5 ± 0.3*	29.2 ± 2.4
Lymph node cells					
WT	31.5 ± 3.5	22.2 ± 1.6	48.8 ± 1.8		13.9 ± 2.3
$P2X_7R^{-/-}$	27.7 ± 0.4	18.5 ± 0.9	51.1 ± 0.9		8.8 ± 0.5
Spleen cells					
WT	24.2 ± 0.4	13.8 ± 0.2	48.6 ± 3.2	13.7 ± 4.8	14.7 ± 3.8
$P2X_7R^{-/-}$	22.0 ± 0.7	11.2 ± 1.1	56.7 ± 2.4	9.5 ± 0.4	9.6 ± 0.7

[a] All values are presented as the mean ± SD percentage of each cell type ($n = 3$ per group).
$*$, $p < 0.05$ (between WT and $P2X_7R^{-/-}$ animals).

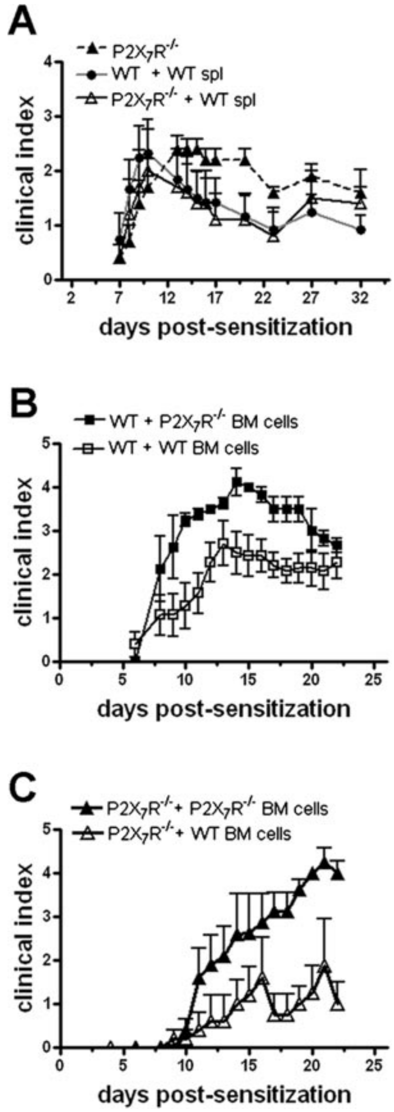

FIGURE 3. Spleen cell transfer and BM chimeras revealed a role for $P2X_7R^{-/-}$ leukocytes in disease exacerbation. *A*, WT spleen (spl) cells (20×10^6) were injected i.p. into $P2X_7R^{-/-}$ ($n = 5$, △) and WT mice ($n = 5$, ●) 6 days before active immunization with MOG_{35-55} peptide. $P2X_7R^{-/-}$ mice were sensitized at the same time ($n = 5$, ▲). *B* and *C*, EAE was induced with MOG_{35-55} peptide in BM chimeras, *B*, WT host animals receiving either $P2X_7R^{-/-}$ BM cells (■) or WT BM cells (□). *C*, $P2X_7R^{-/-}$ animals receiving $P2X_7R^{-/-}$ BM cells (▲) or WT BM cells (△). Clinical scores were assessed daily, and data shown as mean ± SD ($n = 6$ per group).

mRNA levels for IL-1 were significantly lower in spinal cord homogenates from $P2X_7R^{-/-}$ EAE mice as compared with samples from WT animals.

To determine whether purified $CD4^+$ T cells from $P2X_7R^{-/-}$ mice also showed an increased proliferative response to MOG, CD4 cells were isolated from spleens of MOG-sensitized WT and $P2X_7R^{-/-}$ mice at three different time points using magnetic beads. As APCs, DCs were prepared from BM of adult nonsensitized WT and $P2X_7R^{-/-}$ mice using GM-CSF (see *Materials and Methods*). In these cultures, DCs from WT and $P2X_7R^{-/-}$ mice did not show any difference in expression of MHC class II, B7.1, or B7.2 (data not shown). We then performed a mix and match proliferation experiment as described in *Materials and Methods*. No significant difference was detected in the proliferation index between WT and $P2X_7R^{-/-}$ cell populations (data not shown). Similarly, analysis of IFN-γ levels (Fig. 4*E*) and NO production (data not shown) from these cultures of purified CD4 cells showed no difference between WT and $P2X_7R^{-/-}$ cells. These data show that reduced IFN-γ production is not an intrinsic property of Ag-reactive T cells in the $P2X_7R^{-/-}$ mice.

The incidence of apoptosis in the CNS of sensitized animals is higher in WT than in $P2X_7R^{-/-}$ mice

The experiments described above suggested that the cytolytic activity of the $P2X_7R$ in lymphocytes plays a role in regulating EAE. To determine whether a difference in cells undergoing cell death could be detected in vivo between WT and $P2X_7R^{-/-}$ mice, cells were isolated from the CNS on day 7, stained for annexin V and PI, and analyzed by FACS. The lymphocyte gate was determined by staining for CD3. The results (Fig. 5*A*) showed that more cells displayed evidence of cell death in samples derived from the CNS of WT animals than from $P2X_7R^{-/-}$ animals. Cumulative data from four additional experiments for both the total mononuclear cell population isolated from the CNS (day 7), as well as for cells within the lymphocyte gate, are shown in Fig. 5*C*.

We then performed TUNEL staining on sections derived from animals sensitized 11 days earlier. In agreement with previously published data (43), in both the brain and spinal cord the majority of apoptotic cells in these tissues were localized to perivascular infiltrates. In these tissues, more TUNEL-positive cells were detected in inflammatory lesions in WT animals than in $P2X_7R^{-/-}$ animals (Fig. 5*E*). Quantification of these data is shown in Fig. 5*F*. Furthermore, CD3 and DAPI immunohistochemistry staining in WT EAE brain tissues confirmed that apoptotic cells within the perivascular cuffs included $CD3^+$ T cells (Fig. 5*G*).

It has been proposed that recovery from the acute clinical episode in EAE is associated with apoptotic events in activated lymphocytes in the CNS (44). Therefore, to determine whether any differences were detected between WT and $P2X_7R^{-/-}$ mice during this phase of EAE, we used the same assays described above on samples harvested on day 14 postsensitization. The results showed no difference in the percentage of cells undergoing cell death as determined by FACS analysis (Fig. 5*B*) or TUNEL staining (Fig. 5*G*) at this time point.

FACs analysis of lymphocyte expression of ART2.2 in EAE

It has been shown that in lymphocytes the $P2X_7R$ can mediate apoptosis induced by extracellular NAD through an interaction with ART 2.2 (28). This enzyme is known to be expressed only in T cells and to be shed upon activation (45). To explore the possibility that ART2.2 expression might correlate with apoptotic activity in lymphocytes in these mice, we assessed ART2.2 expression by FACS in lymphocytes isolated from the CNS, spleen, and lymph nodes 7 and 14 days postsensitization with MOG. The results showed no difference in the percentage of lymphocytes that expressed ART 2.2 between WT and $P2X_7R^{-/-}$ mice (Fig. 6). However, in cells isolated from the CNS, the percentage of $CD3^+$ T cells that expressed ART2.2 was lower than in spleen and lymph node populations. This difference was particularly striking in males for both day 7 and day 14. This would suggest that in males more of the lymphocytes in the CNS are in an activated state than in females.

Discussion

In this study we have shown that mice lacking a functional $P2X_7R$ are more susceptible to MOG-induced EAE than their WT counterparts. Clinical expression of disease was more severe during

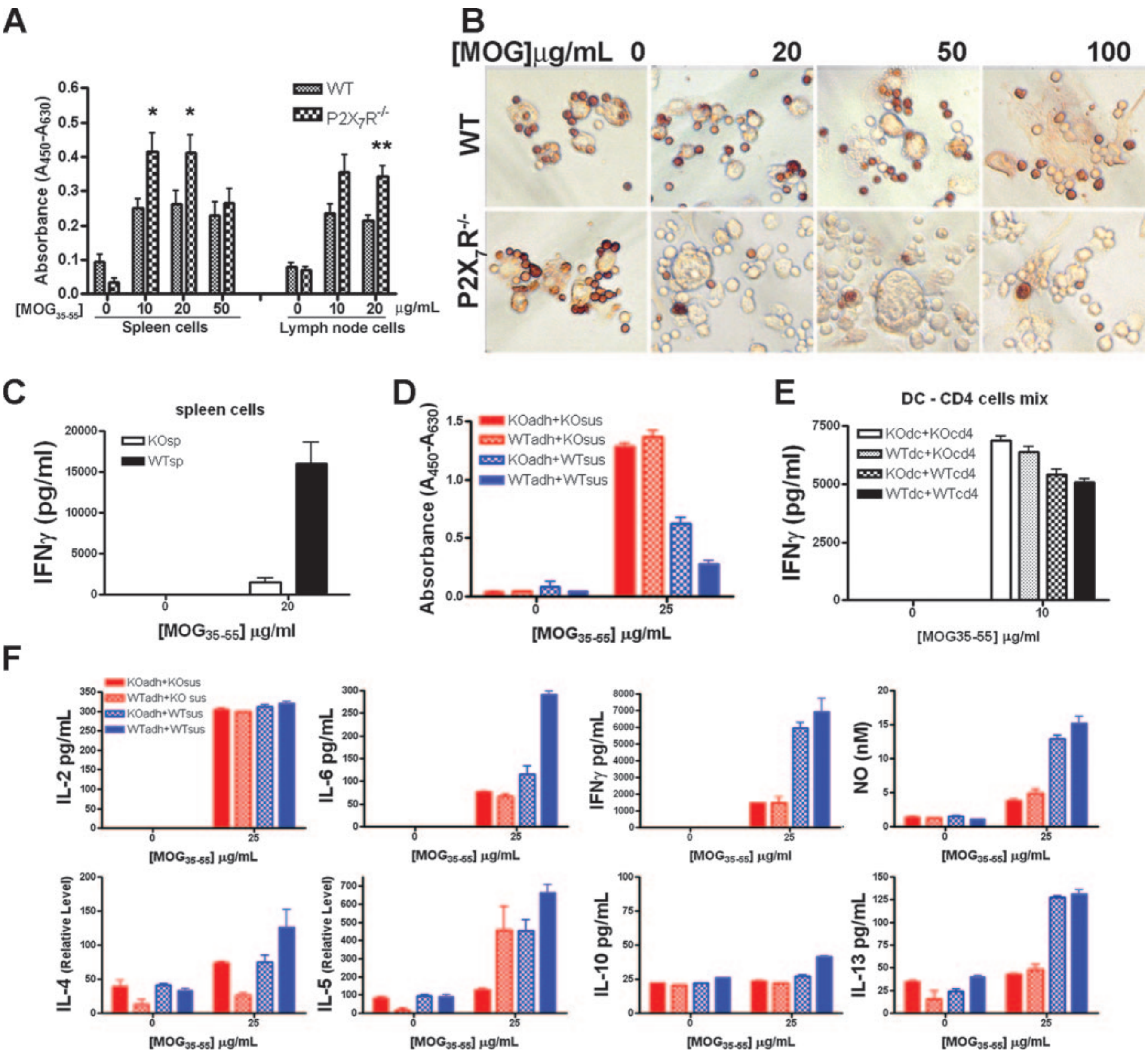

FIGURE 4. Immune response to MOG in spleen and lymph node cells of WT and $P2X_7R^{-/-}$ mice. *A*, Spleen and lymph node cells were harvested on day 7 from WT and $P2X_7R^{-/-}$ mice and stimulated with $MOG_{35–55}$ peptide at the indicated concentrations. Proliferation was determined using BrdU (n = 7 mice per group; $*$, $p < 0.05$). *B*, TUNEL staining was performed to determine the cytotoxic response in spleen cells cultured as in *A*. The majority of the apoptotic cells in these cultures were lymphocytes. *C*, IFN-γ levels, as determined by ELISA, in supernatants harvested from spleen (sp) cells cultured with or without MOG (20 μg/ml) from experiment in *A*. *D*, Spleen cells were prepared from WT and $P2X_7R^{-/-}$ mice sensitized with $MOG_{35–55}$ peptide. Nonadherent spleen cells were transferred from WT mice onto adherent cells from $P2X_7R^{-/-}$ mice and vice versa. Control cultures consisting of WT, WT and $P2X_7R^{-/-}$, and $P2X_7R^{-/-}$ were prepared in parallel. Cells were cultured with 25 μg/ml $MOG_{35–55}$ peptide for 5 days, and a proliferation assay was performed using BrdU. One of four experiments is shown. *E*, IFN-γ production of culture supernatants from the mix and match cultures using purified DC (dc) and CD4 (cd4) cells was measured using an ELISA kit. *F*, Cytokine and NO production of culture supernatant harvested from the experiment shown in *C* was determined using FAST Quant mouse Th1/Th2 kit and the Griess reaction.

both the acute and the chronic phases of the disease, and pathological examination of the tissues showed that the typical inflammatory and destructive lesions in the CNS were more widespread in $P2X_7R^{-/-}$ mice than in WT mice. Of particular note was the more extensive involvement of the brain. EAE is known to initially affect the more distal regions of the cord and to involve more proximal regions with time and increased severity. Therefore, more numerous perivascular lesions in the brain reflect a more severe inflammatory process in the $P2X_7R^{-/-}$ mice. Radiation BM chimeras showed that increased susceptibility to EAE resided within the BM-derived cells, indicating that radiation-resistant cells within the CNS did not confer susceptibility to EAE in the $P2X_7R^{-/-}$ mice, at least for the acute phase of the disease. In vitro, proliferation assays and TUNEL staining showed that spleen and lymph node cells from $P2X_7R^{-/-}$ mice had a higher proliferative activity in response to MOG peptide and that lymphocytes in these cultures showed less evidence of apoptosis. Mixed transfer experiments of spleen adherent and nonadherent cells indicated that adherent cells were not a major source of factors regulating lymphocyte proliferation and/or cell death. Annexin V/PI staining of CNS-infiltrating cells also revealed that there were fewer apoptotic cells in the CNS of $P2X_7R^{-/-}$ mice than in that of WT mice, and TUNEL staining of sections of brain and

Table III. *Cytokine mRNA and protein expression in spinal cord homogenates from EAE mice*[a]

	IL-1β	IL-6	TNFα	IL-2	IFN-γ	IL-4
QPCR[b]						
WT	179 ± 14	25 ± 2	58 ± 11	ND[c]	26 ± 3	ND[c]
$P2X_7R^{-/-}$	152 ± 15	16 ± 2*	62 ± 26	ND[c]	9 ± 0.8***	ND[c]
Protein						
WT	808 ± 96	851 ± 111	265 ± 20	267 ± 28	305 ± 33	96 ± 10
$P2X_7R^{-/-}$	348 ± 54***	416 ± 55**	232 ± 29	217 ± 33	211 ± 33	89 ± 22

[a] Data are expressed as mean ± SD of the relative expression levels for four animals per group harvested on day 9.
[b] Quantitative PCR.
[c] Not done.
*, $p < 0.05$ (between WT and $P2X_7R^{-/-}$ animals).
**, $p < 0.01$ (between WT and $P2X_7R^{-/-}$ animals).
***, $p < 0.001$ (between WT and $P2X_7R^{-/-}$ animals).

spinal cord gave the same result. These data are the first to show that the $P2X_7R$ regulates T cell-mediated inflammation of the CNS and support an important role for this receptor in lymphocyte homeostasis.

The contribution of the $P2X_7R$ to inflammation and the immune response was first recognized following the identification of its role in the processing and release of IL-1 (3, 5). Consistent with this function for the $P2X_7R$, we noted that whereas mRNA for IL-1 did not differ in spinal cord homogenates from $P2X_7R^{-/-}$ mice and WT mice, protein assays showed a significant reduction in IL-1 levels in the $P2X_7R^{-/-}$ mouse. In many cell types, activation with IL-1 leads to the induction of IL-6; thus, the reduced levels of both mRNA and protein detected in spinal cord homogenates for IL-6 in the $P2X_7R^{-/-}$ mice would also be consistent with a reduction in the levels of IL-1 in these mice. Both IL-1 and IL-6 are well recognized as proinflammatory cytokines, are elevated in the early stages of EAE, and are considered risk factors for EAE (46–48); therefore, the reduced levels of both IL-1 and IL-6 in the $P2X_7R^{-/-}$ mouse are at variance with their known role in this disease. However, these cytokines also have immunosuppressive functions, and their expression in the CNS has been shown to assist in recovery and repair following toxic or traumatic insults to the brain (49–51). Neuronal/axonal injury has only recently been recognized as a component of clinical expression of EAE, and both IL-1 and IL-6 may contribute to the recovery from the acute clinical episode by offering protection against destruction of these tissues. Thus, in common with TNF and IFN-γ, IL-1 and IL-6 likely play complex roles in the clinical and pathological expression of EAE (47, 48, 52).

Our data strongly implicate loss of apoptotic activity in lymphocytes as a contributing factor to disease exacerbation in the $P2X_7R^{-/-}$ mouse. In the EAE model, several studies have proposed that Ag-induced cell death in the CNS contributes to the recovery from the acute phase of the disease (44), and both Fas/FasL interactions (53–55) and p53 (56) have been implicated in this process. The observation that the frequency of apoptotic events in the CNS only differed between $P2X_7R^{-/-}$ and WT mice during the early phases of the disease suggests that $P2X_7R$-dependent apoptosis may be one of several death-inducing pathways that become activated in the inflamed CNS, forming part of a complex immunoregulatory process that evolves over the course of the disease. The mechanism by which the $P2X_7R$ regulates apoptosis in lymphocytes requires further investigation, but decreased apoptotic activity of $P2X_7R^{-/-}$ lymphocytes correlated with reduced levels of IFN-γ and NO in supernatants from Ag-activated cultures. Reduced levels of IFN-γ were also noted in spinal cord homogenates from $P2X_7R^{-/-}$ mice with EAE when compared with WT controls. These data are consistent with several previous studies that have clearly linked a role for IFN-γ and NO as regulatory factors in EAE (57–59). In this scenario, high levels of NO are generated by the inducible form of NO synthase, which is potently activated in macrophages, as well as in other cell types, by IFN-γ (59). NO then acts to induce T cell apoptosis and to block T cell proliferation, thus functioning to limit the expansion of autoreactive T cells.

However, we did not detect any difference in the MOG-induced proliferative activity of WT and $P2X_7R^{-/-}$ lymphocytes when purified DC and CD4 cells were used to perform the mix and match culture experiments. Similarly, no difference in the production of IFN-γ and NO was detected (Fig. 4*E*, and data not shown). These data indicate that $P2X_7R^{-/-}CD4^+$ T cells from MOG sensitized animal are fully capable of making IFN-γ in response to MOG when separated from other spleen cells. Thus, the decreased production of IFN-γ found in $P2X_7R^{-/-}$ spleen cells in the in vitro cultures (Figs. 4, *C* and *F*), as well as in the spinal cord homogenates (Table III), suggest the presence of a regulatory cell(s) or factor that inhibits the production of IFN-γ. In this regard, it is of interest to note that $P2X_7R^{-/-}$ mice have recently been reported to have enhanced FoxP3 and $CD4^+CD25^+$ regulatory T cell activity (30), and our unpublished data for FoxP3 expression in $P2X_7R^{-/-}$ EAE mice is consistent with this finding, suggesting no role for this type of T regulatory cell in this process. However, whether some other possible regulatory cell is involved in this processing, e.g., $CD8^+$ T cells, B cells, γδ T cells, or NK cells, remains to be determined.

Decreased apoptosis of lymphocytes in $P2X_7R^{-/-}$ mice also likely reflects a direct role for the $P2X_7R$ in mediating cell death. In most cell types, ligand binding to the $P2X_7R$ results in two conductance states: following brief exposure to ligands such as ATP a nonselective cation channel is activated, but following prolonged or repeated exposure to high dose ATP a large macromolecular pore is formed. These changes result in transmembrane ion flux (particularly influx of Ca^{2+}, Na^+, and efflux of K^+), cell swelling, vacuolation, and death by both necrotic and apoptotic means. There are multiple potential sources of high levels of ATP in the inflamed CNS; however, it could be questioned whether ATP is the specific ligand involved in these experiments. In mice, a single base pair substitution, T1352C (P451L), has been detected in the $P2X_7R$ genome that dramatically affects receptor function. This mutation lies within a region of the C-terminal cytoplasmic tail that bears significant homology with a TNFR1 death domain, as well as to a fragment of the Src homology 3-binding protein (60, 61). Different strains of mice carry different alleles of the $P2X_7R$, with the *L451* allele conferring a reduced sensitivity to ATP-induced channel activity and pore formation (60, 61). C57BL/6 mice express this allele, and T cells from these mice show reduced apoptotic activity to ATP when compared with T cells from BALB/c

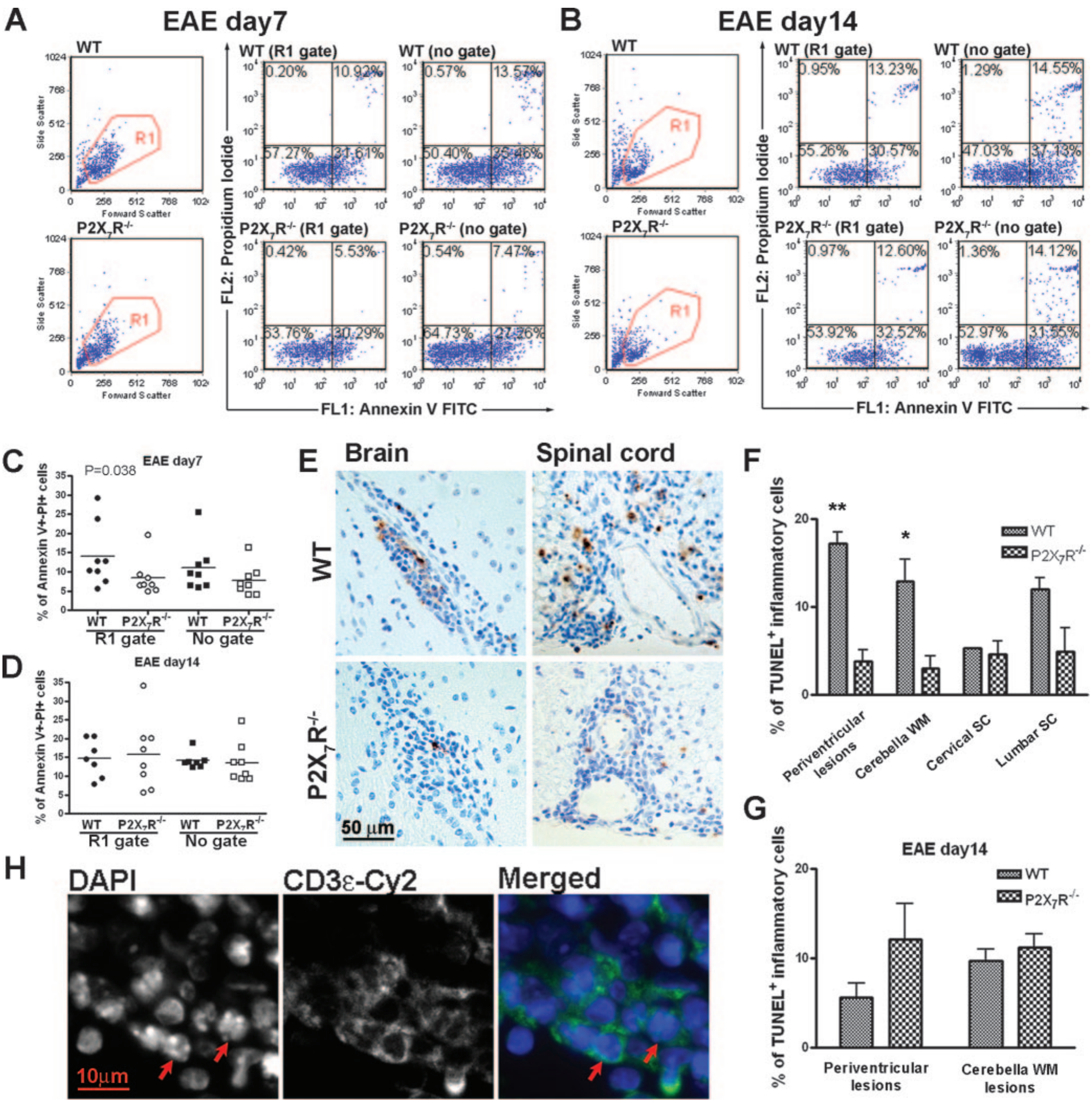

FIGURE 5. The incidence of apoptosis in the CNS of sensitized mice is higher in WT mice than $P2X_7R^{-/-}$ mice. *A* and *B*, Infiltrating mononuclear cells were isolated from the CNS of $P2X_7R^{-/-}$ and WT mice on day 7 (*A*) and day14 (*B*) postsensitization with MOG, and cells were stained for annexin V and PI. The lymphocyte gate was determined by staining for CD3. *C* and *D*, Cumulative FACS data for CNS infiltrating mononuclear cells stained for annexin V and PI on day 7 (*C*) and day14 (*D*). Each symbol represents data from one mouse. Data were significantly different between $P2X_7R^{-/-}$ mice and WT for day 7 but not for day 14 ($p < 0.04$). *E*, TUNEL staining was performed on brain or spinal cord sections derived from animals sensitized 11 days previously. *F*, The cumulative data for the percentage of TUNEL-positive inflammatory cells for tissue harvested on days 11 and 14. Asterisk denotes values significantly different from the $P2X_7R^{-/-}$ mice: **, $p < 0.001$, *, $p < 0.05$, $n = 6$ per group. *H*, Immunofluorescence staining of CD3ϵ and DAPI is shown in an inflammatory lesion from brain sections of a WT EAE mouse. Red arrows indicate the apoptotic cells with condensed chromatin that are double-stained for CD3ϵ.

mice. More recently, an alternative $P2X_7R$-dependent cell death pathway in T cells has been proposed that is induced by NAD acting as a substrate for the cell surface ART2 (28). Binding of covalently attached ADP-ribosyl groups to the $P2X_7R$ results in pore formation and rapid cell death following exposure to much lower concentrations of NAD than of ATP (29). These data prompted us to study ART2 expression in $CD3^+$ T cells isolated from the CNS, spleen, and lymph node at varying times in the disease process (Fig. 6). No differences were observed between WT and $P2X_7R^{-/-}$ mice in any of these samples. However, strikingly lower percentages of $CD3^+ART2^+$ cells were isolated from the inflamed CNS than from spleen and lymph nodes, especially in males. Because ART2 is rapidly shed from the T cell surface following activation, these data indicate that a much higher percentage of T cells in the CNS are activated compared with lymphocytes in peripheral lymphoid organs and further suggest that the

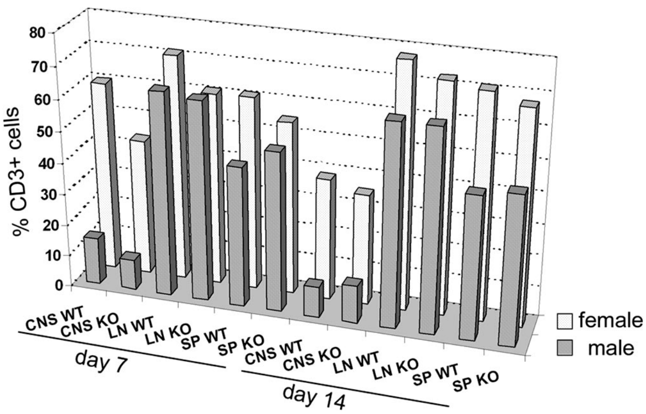

FIGURE 6. Lymphocyte expression of ART2.2 in EAE. CNS-infiltrating mononuclear cells, lymph node (LN) cells, and spleen (SP) cells were isolated from WT and $P2X_7R^{-/-}$ mice on days 7 and 14 postsensitization with MOG for both males and females. ART2.2 expression level in T cells was determined by FACS using double-staining for ART2.2 and CD3. Data are expressed as the mean value of three mice per group. SD values were within 10%.

more severe disease noted in males may reflect a higher and more prolonged state of activation of $CD3^+$ cells in the CNS than that found in females.

Interestingly, although the clinical course of EAE was more severe in male WT mice than in female WT mice, we found little difference in disease activity between $P2X_7R^{-/-}$ males and $P2X_7R^{-/-}$ females. These data suggest that there may be an interaction between sex steroids and signaling via the $P2X_7R$. Consistent with this hypothesis, it has been shown in vitro that 17β-estradiol and estrogen regulate receptor activation when assessed by electrophysiological methods (62, 63), and studies in vivo that have addressed a role for this receptor in bone formation and resorption found a greater reduction in bone formation in male $P2X_7R^{-/-}$ mice as compared with normal controls than in female $P2X_7R^{-/-}$ vs WT mice (64). These results suggest that certain sex related molecules may regulate the function of the $P2X_7R$ and that, in the absence of this receptor, this effect disappears.

It should be noted here that the more severe disease seen in males in these experiments is at variance with previously published data for C57BL6 mice where no difference in susceptibility to EAE between males and females was noted (65, 66) but is consistent with sex differences in susceptibility to EAE in other strains of mice (66). Although we have no explanation for this result at the present time, we did observe that the C57BL/6NTac mice, when sensitized side-by-side with C57BL/6J mice, were less sensitive to MOG-EAE induction. Thus, our data likely reflect a genetic drift that has occurred in these substrains over the extended length of time that these mice have been inbred, as has been noted previously for BL6 mice (67).

Like the mouse, several polymorphisms have also been detected in the human $P2X_7R$ that affect receptor function (68, 69). The best studied of these is the A1513C (E496A) variant, which also resides within a region of the C-terminal tail that shows homology with the TNFR1 death domain (68). Individuals with the 1513C genotype show a loss-of-function for the $P2X_7R$ with respect to both pore formation and cytokine production (68–71). Several studies have also suggested an association between this polymorphism and patients with B cell chronic lymphocytic leukemia (CLL) (72–76). At the present time the exact contribution that this receptor plays to disease expression in CLL remains to be resolved; but, as has been cogently discussed by Di Virgilio and Wiley (76), the data could equally well be interpreted to support either a growth promoting activity for the receptor, a loss of apoptotic activity, and/or a loss of regulation of adhesion molecules important in facilitating B cell exit from the peripheral circulation. Nevertheless, taken together these data support a role for this receptor in clinical manifestations of disease in patients with CLL.

Understanding the pathogenesis of inflammation is a central issue in furthering our understanding of a wide range of human diseases. Activation of the inflammatory response is recognized to be an essential component of an effective defense against microbial infections but also raises the danger of inducing irreversible tissue damage, as well as possibly activating autoreactive bystander T cells (28). The $P2X_7R$ is emerging as a central regulator of the inflammatory process, but little is known about how this receptor functions in different models of inflammation in vivo. The data presented here, along with the data previously reported by Labasi et al. (20) and Chessell et al. (22), show that the $P2X_7R$ differentially regulates inflammation depending upon the underlying mechanisms involved, i.e. it attenuates disease elicited by a combination of Ab and the TLR4 ligand LPS (20) and chronic inflammatory and neuropathic pain (22), but it exacerbates disease mediated by $CD4^+$ T cells. It is of particular interest to note that these four models were tested in the same C57BL/6 mouse strain that expresses a receptor with low affinity for ATP; therefore, it will be of further interest to test different models of inflammation in $P2X_7R^{-/-}$ mice back-crossed onto other strains of mice. Because certain polymorphisms in the human $P2X_7R$ have also been found to have functional consequences and to associate with disease, this mouse model provides a valuable tool for furthering our understanding of the complex role of the $P2X_7R$ in inflammation.

Acknowledgments

We thank Dr. Christopher A. Gabel (current address Amgen, Seattle, WA) and Pfizer (Groton, CT) for providing the $P2X_7R^{-/-}$ mice, Dr. Cedric S. Raine (Albert Einstein College of Medicine, Bronx, NY) for assistance with the pathology, and Dr. Laura Santambrogio (Albert Einstein College of Medicine) for assistance with the dendritic cell cultures and for critical reading of the manuscript.

Disclosures

The authors have no financial conflict of interest.

References

1. Burnstock, G., and M. Williams. 2000. P2 purinergic receptors: modulation of cell function and therapeutic potential. *J. Pharmacol. Exp. Ther.* 295: 862–869.
2. Surprenant, A., F. Rassendren, E. Kawashima, R. A. North, and G. Buell. 1996. The cytolytic P2Z receptor for extracellular ATP identified as a P2X receptor (P2X7). *Science* 272: 735–738.
3. Chessell, I. P., J. Simon, A. D. Hibell, A. D. Michel, E. A. Barnard, and P. P. Humphrey. 1998. Cloning and functional characterisation of the mouse P2X7 receptor. *FEBS Lett.* 439: 26–30.
4. Smart, M. L., B. Gu, R. G. Panchal, J. Wiley, B. Cromer, D. A. Williams, and S. Petrou. 2003. P2X7 receptor cell surface expression and cytolytic pore formation are regulated by a distal C-terminal region. *J. Biol. Chem.* 278: 8853–8860.
5. Di Virgilio, F., P. Chiozzi, D. Ferrari, S. Falzoni, J. M. Sanz, A. Morelli, M. Torboli, G. Bolognesi, and O. R. Baricordi. 2001. Nucleotide receptors: an emerging family of regulatory molecules in blood cells. *Blood* 97: 587–600.
6. Ferrari, D., P. Chiozzi, S. Falzoni, S. Hanau, and F. Di Virgilio. 1997. Purinergic modulation of interleukin-1 β release from microglial cells stimulated with bacterial endotoxin. *J. Exp. Med.* 185: 579–582.
7. Ferrari, D., P. Chiozzi, S. Falzoni, M. Dal Susino, L. Melchiorri, O. R. Baricordi, and F. Di Virgilio. 1997. Extracellular ATP triggers IL-1 β release by activating the purinergic P2Z receptor of human macrophages. *J. Immunol.* 159: 1451–1458.
8. Suzuki, T., I. Hide, K. Ido, S. Kohsaka, K. Inoue, and Y. Nakata. 2004. Production and release of neuroprotective tumor necrosis factor by P2X7 receptor-activated microglia. *J. Neurosci.* 24: 1–7.
9. Kucher, B. M., and J. T. Neary. 2005. Bi-functional effects of ATP/P2 receptor activation on tumor necrosis factor-α release in lipopolysaccharide-stimulated astrocytes. *J Neurochem.* 92: 525–535.

10. Baricordi, O. R., L. Melchiorri, E. Adinolfi, S. Falzoni, P. Chiozzi, G. Buell, and F. Di Virgilio. 1999. Increased proliferation rate of lymphoid cells transfected with the $P2X_7$ ATP receptor. *J. Biol. Chem.* 274: 33206–33208.
11. Budagian, V., E. Bulanova, L. Brovko, Z. Orinska, R. Fayad, R. Paus, and S. Bulfone-Paus. 2003. Signaling through P2X7 receptor in human T cells involves $p56^{lck}$, MAP kinases, and transcription factors AP-1 and NF-κB. *J. Biol. Chem.* 278: 1549–1560.
12. Chiozzi, P., J. M. Sanz, D. Ferrari, S. Falzoni, A. Aleotti, G. N. Buell, G. Collo, and F. Di Virgilio. 1997. Spontaneous cell fusion in macrophage cultures expressing high levels of the P2Z/P2X7 receptor. *J. Cell Biol.* 138: 697–706.
13. Di Virgilio, F., S. Falzoni, P. Chiozzi, J. M. Sanz, D. Ferrari, and G. N. Buell. 1999. ATP receptors and giant cell formation. *J. Leukocyte Biol.* 66: 723–726.
14. Lammas, D. A., C. Stober, C. J. Harvey, N. Kendrick, S. Panchalingam, and D. S. Kumararatne. 1997. ATP-induced killing of mycobacteria by human macrophages is mediated by purinergic P2Z(P2X7) receptors. *Immunity* 7: 433–444.
15. Coutinho-Silva, R., J. L. Perfettini, P. M. Persechini, A. Dautry-Varsat, and D. M. Ojcius. 2001. Modulation of P2Z/P2X(7) receptor activity in macrophages infected with *Chlamydia psittaci*. *Am. J. Physiol.* 280: C81–C89.
16. Kusner, D. J., and J. Adams. 2000. ATP-induced killing of virulent *Mycobacterium tuberculosis* within human macrophages requires phospholipase D. *J. Immunol.* 164: 379–388.
17. Hu, Y., P. L. Fisette, L. C. Denlinger, A. G. Guadarrama, J. A. Sommer, R. A. Proctor, and P. J. Bertics. 1998. Purinergic receptor modulation of lipopolysaccharide signaling and inducible nitric oxide synthase expression in RAW 264.7 macrophages. *J. Biol. Chem.* 273: 27170–27175.
18. Gendron, F. P., M. Chalimoniuk, J. Strosznajder, S. Shen, F. A. Gonzalez, G. A. Weisman, and G. Y. Sun. 2003. P2X7 nucleotide receptor activation enhances IFN-γ-induced type II nitric oxide synthase activity in BV-2 microglial cells. *J. Neurochem.* 87: 344–352.
19. Gu, B., L. J. Bendall, and J. S. Wiley. 1998. Adenosine triphosphate-induced shedding of CD23 and L-selectin (CD62L) from lymphocytes is mediated by the same receptor but different metalloproteases. *Blood* 92: 946–951.
20. Labasi, J. M., N. Petrushova, C. Donovan, S. McCurdy, P. Lira, M. M. Payette, W. Brissette, J. R. Wicks, L. Audoly, and C. A. Gabel. 2002. Absence of the P2X7 receptor alters leukocyte function and attenuates an inflammatory response. *J. Immunol.* 168: 6436–6445.
21. Solle, M., J. Labasi, D. G. Perregaux, E. Stam, N. Petrushova, B. H. Koller, R. J. Griffiths, and C. A. Gabel. 2001. Altered cytokine production in mice lacking P2X(7) receptors. *J. Biol. Chem.* 276: 125–132.
22. Chessell, I. P., J. P. Hatcher, C. Bountra, A. D. Michel, J. P. Hughes, P. Green, J. Egerton, M. Murfin, J. Richardson, W. L. Peck, C. B. Grahames, M. A. Casula, Y. Yiangou, R. Birch, P. Anand, and G. N. Buell. 2005. Disruption of the P2X7 purinoceptor gene abolishes chronic inflammatory and neuropathic pain. *Pain* 114: 386–396.
23. Humphreys, B. D., J. Rice, S. B. Kertesy, and G. R. Dubyak. 2000. Stress-activated protein kinase/JNK activation and apoptotic induction by the macrophage P2X7 nucleotide receptor. *J. Biol. Chem.* 275: 26792–26798.
24. Brough, D., R. A. Le Feuvre, Y. Iwakura, and N. J. Rothwell. 2002. Purinergic (P2X7) receptor activation of microglia induces cell death via an interleukin-1-independent mechanism. *Mol. Cell. Neurosci.* 19: 272–280.
25. Mantuano-Barradas, M., A. Henriques-Pons, T. C. Araujo-Jorge, F. Di Virgilio, R. Coutinho-Silva, and P. M. Persechini. 2003. Extracellular ATP induces cell death in $CD4^+/CD8^+$ double-positive thymocytes in mice infected with *Trypanosoma cruzi*. *Microbes Infect.* 5: 1363–1371.
26. Klapperstuck, M., C. Buttner, T. Bohm, G. Schmalzing, and F. Markwardt. 2000. Characteristics of P2X7 receptors from human B lymphocytes expressed in *Xenopus* oocytes. *Biochim. Biophys. Acta* 1467: 444–456.
27. Wiley, J. S., C. E. Gargett, W. Zhang, M. B. Snook, and G. P. Jamieson. 1998. Partial agonists and antagonists reveal a second permeability state of human lymphocyte P2Z/P2X7 channel. *Am. J. Physiol.* 275: C1224–C1231.
28. Seman, M., S. Adriouch, F. Scheuplein, C. Krebs, D. Freese, G. Glowacki, P. Deterre, F. Haag, and F. Koch-Nolte. 2003. NAD-induced T cell death: ADP-ribosylation of cell surface proteins by ART2 activates the cytolytic P2X7 purinoceptor. *Immunity* 19: 571–582.
29. Kawamura, H., F. Aswad, M. Minagawa, K. Malone, H. Kaslow, F. Koch-Nolte, W. H. Schott, E. H. Leiter, and G. Dennert. 2005. P2X7 receptor-dependent and -independent T cell death is induced by nicotinamide adenine dinucleotide. *J. Immunol.* 174: 1971–1979.
30. Aswad, F., H. Kawamura, and G. Dennert. 2005. High sensitivity of $CD4^+CD25^+$ regulatory T cells to extracellular metabolites nicotinamide adenine dinucleotide and ATP: a role for P2X7 receptors. *J. Immunol.* 175: 3075–3083.
31. Wekerle, H., K. Kojima, J. Lannes-Vieira, H. Lassmann, and C. Linington. 1994. Animal models. *Ann. Neurol.* 36(Suppl.): S47–S53.
32. Raine, C. S. 1994. The Dale E. McFarlin memorial lecture: the immunology of the multiple sclerosis lesion. *Ann. Neurol.* 36(Suppl.): S61–S72.
33. Langrish, C. L., Y. Chen, W. M. Blumenschein, J. Mattson, B. Basham, J. D. Sedgwick, T. McClanahan, R. A. Kastelein, and D. J. Cua. 2005. IL-23 drives a pathogenic T cell population that induces autoimmune inflammation. *J. Exp. Med.* 201: 233–240.
34. Park, H., Z. Li, X. O. Yang, S. H. Chang, R. Nurieva, Y. H. Wang, Y. Wang, L. Hood, Z. Zhu, Q. Tian, and C. Dong. 2005. A distinct lineage of CD4 T cells regulates tissue inflammation by producing interleukin 17. *Nat. Immunol.* 6: 1133–1141.
35. Harrington, L. E., R. D. Hatton, P. R. Mangan, H. Turner, T. L. Murphy, K. M. Murphy, and C. T. Weaver. 2005. Interleukin 17-producing $CD4^+$ effector T cells develop via a lineage distinct from the T helper type 1 and 2 lineages. *Nat. Immunol.* 6: 1123–1132.
36. Mannie, M. D., C. A. Dinarello, and P. Y. Paterson. 1987. Interleukin 1 and myelin basic protein synergistically augment adoptive transfer activity of lymphocytes mediating experimental autoimmune encephalomyelitis in Lewis rats. *J. Immunol.* 138: 4229–4235.
37. Probert, L., H. P. Eugster, K. Akassoglou, J. Bauer, K. Frei, H. Lassmann, and A. Fontana. 2000. TNFR1 signaling is critical for the development of demyelination and the limitation of T-cell responses during immune-mediated CNS disease. *Brain* 123: 2005–2019.
38. Le Feuvre, R. A., D. Brough, Y. Iwakura, K. Takeda, and N. J. Rothwell. 2002. Priming of macrophages with lipopolysaccharide potentiates P2X7-mediated cell death via a caspase-1-dependent mechanism, independently of cytokine production. *J. Biol. Chem.* 277: 3210–3218.
39. Rajan, A. J., Y. L. Gao, C. S. Raine, and C. F. Brosnan. 1996. A pathogenic role for $\gamma\delta$ T cells in relapsing-remitting experimental allergic encephalomyelitis in the SJL mouse. *J. Immunol.* 157: 941–949.
40. Rivieccio, M. A., G. R. John, X. Song, H. S. Suh, Y. Zhao, S. C. Lee, and C. F. Brosnan. 2005. The cytokine IL-1β activates IFN response factor 3 in human fetal astrocytes in culture. *J. Immunol.* 174: 3719–3726.
41. Liu, J. S., M. L. Zhao, C. F. Brosnan, and S. C. Lee. 2001. Expression of inducible nitric oxide synthase and nitrotyrosine in multiple sclerosis lesions. *Am. J. Pathol.* 158: 2057–2066.
42. Le Feuvre, R., D. Brough, and N. Rothwell. 2002. Extracellular ATP and P2X7 receptors in neurodegeneration. *Eur. J. Pharmacol.* 447: 261–269.
43. Bonetti, B., J. Pohl, Y. L. Gao, and C. S. Raine. 1997. Cell death during autoimmune demyelination: effector but not target cells are eliminated by apoptosis. *J. Immunol.* 159: 5733–5741.
44. Tabi, Z., P. A. McCombe, and M. P. Pender. 1995. Antigen-specific down-regulation of myelin basic protein-reactive T cells during spontaneous recovery from experimental autoimmune encephalomyelitis: further evidence of apoptotic deletion of autoreactive T cells in the central nervous system. *Int. Immunol.* 7: 967–973.
45. Kahl, S., M. Nissen, R. Girisch, T. Duffy, E. H. Leiter, F. Haag, and F. Koch-Nolte. 2000. Metalloprotease-mediated shedding of enzymatically active mouse ecto-ADP-ribosyltransferase ART2.2 upon T cell activation. *J. Immunol.* 165: 4463–4469.
46. Schiffenbauer, J., W. J. Streit, E. Butfiloski, M. LaBow, C. Edwards III, and L. L. Moldawer. 2000. The induction of EAE is only partially dependent on TNF receptor signaling but requires the IL-1 type I receptor. *Clin. Immunol.* 95: 117–123.
47. Ishihara, K., and T. Hirano. 2002. IL-6 in autoimmune disease and chronic inflammatory proliferative disease. *Cytokine Growth Factor Rev.* 13: 357–368.
48. Wang, J., V. C. Asensio, and I. L. Campbell. 2002. Cytokines and chemokines as mediators of protection and injury in the central nervous system assessed in transgenic mice. *Curr. Top. Microbiol. Immunol.* 265: 23–48.
49. Mason, J. L., K. Suzuki, D. D. Chaplin, and G. K. Matsushima. 2001. Interleukin-1β promotes repair of the CNS. *J. Neurosci.* 21: 7046–7052.
50. Penkowa, M., M. Giralt, N. Lago, J. Camats, J. Carrasco, J. Hernandez, A. Molinero, I. L. Campbell, and J. Hidalgo. 2003. Astrocyte-targeted expression of IL-6 protects the CNS against a focal brain injury. *Exp. Neurol.* 181: 130–148.
51. Swartz, K. R., F. Liu, D. Sewell, T. Schochet, I. Campbell, M. Sandor, and Z. Fabry. 2001. Interleukin-6 promotes post-traumatic healing in the central nervous system. *Brain Res.* 896: 86–95.
52. Linker, R. A., M. Sendtner, and R. Gold. 2005. Mechanisms of axonal degeneration in EAE: lessons from CNTF and MHC I knockout mice. *J. Neurol. Sci.* 233: 167–172.
53. Suvannavejh, G. C., M. C. Dal Canto, L. A. Matis, and S. D. Miller. 2000. Fas-mediated apoptosis in clinical remissions of relapsing experimental autoimmune encephalomyelitis. *J. Clin. Invest.* 105: 223–231.
54. Sabelko-Downes, K. A., A. H. Cross, and J. H. Russell. 1999. Dual role for Fas ligand in the initiation of and recovery from experimental allergic encephalomyelitis. *J. Exp. Med.* 189: 1195–1205.
55. Kohji, T., and Y. Matsumoto. 2000. Coexpression of Fas/FasL and Bax on brain and infiltrating T cells in the central nervous system is closely associated with apoptotic cell death during autoimmune encephalomyelitis. *J. Neuroimmunol.* 106: 165–171.
56. Okuda, Y., M. Okuda, and C. C. Bernard. 2003. Regulatory role of p53 in experimental autoimmune encephalomyelitis. *J. Neuroimmunol.* 135: 29–37.
57. Willenborg, D. O., S. A. Fordham, M. A. Staykova, I. A. Ramshaw, and W. B. Cowden. 1999. IFN-γ is critical to the control of murine autoimmune encephalomyelitis and regulates both in the periphery and in the target tissue: a possible role for nitric oxide. *J. Immunol.* 163: 5278–5286.
58. Cowden, W. B., F. A. Cullen, M. A. Staykova, and D. O. Willenborg. 1998. Nitric oxide is a potential down-regulating molecule in autoimmune disease: inhibition of nitric oxide production renders PVG rats highly susceptible to EAE. *J. Neuroimmunol.* 88: 1–8.
59. Willenborg, D. O., M. A. Staykova, and W. B. Cowden. 1999. Our shifting understanding of the role of nitric oxide in autoimmune encephalomyelitis: a review. *J. Neuroimmunol.* 100: 21–35.
60. Adriouch, S., C. Dox, V. Welge, M. Seman, F. Koch-Nolte, and F. Haag. 2002. Cutting edge: a natural P451L mutation in the cytoplasmic domain impairs the function of the mouse P2X7 receptor. *J. Immunol.* 169: 4108–4112.
61. Le Stunff, H., R. Auger, J. Kanellopoulos, and M. N. Raymond. 2004. The Pro-451 to Leu polymorphism within the C-terminal tail of P2X7 receptor impairs cell death but not phospholipase D activation in murine thymocytes. *J. Biol. Chem.* 279: 16918–16926.

62. Cario-Toumaniantz, C., G. Loirand, L. Ferrier, and P. Pacaud. 1998. Nongenomic inhibition of human P2X7 purinoceptor by 17β-oestradiol. *J. Physiol.* 508: 659–666.
63. Wang, Q., X. Li, L. Wang, Y. H. Feng, R. Zeng, and G. Gorodeski. 2004. Antiapoptotic effects of estrogen in normal and cancer human cervical epithelial cells. *Endocrinology* 145: 5568–5579.
64. Ke, H. Z., H. Qi, A. F. Weidema, Q. Zhang, N. Panupinthu, D. T. Crawford, W. A. Grasser, V. M. Paralkar, M. Li, L. P. Audoly, C. A. Gabel, W. S. Jee, S. J. Dixon, S. M. Sims, and D. D. Thompson. 2003. Deletion of the P2X7 nucleotide receptor reveals its regulatory roles in bone formation and resorption. *Mol. Endocrinol.* 17: 1356–1367.
65. Okuda, Y., M. Okuda, and C. C. Bernard. 2002. Gender does not influence the susceptibility of C57BL/6 mice to develop chronic experimental autoimmune encephalomyelitis induced by myelin oligodendrocyte glycoprotein. *Immunol. Lett.* 81: 25–29.
66. Papenfuss, T. L., C. J. Rogers, I. Gienapp, M. Yurrita, M. McClain, N. Damico, J. Valo, F. Song, and C. C. Whitacre. 2004. Sex differences in experimental autoimmune encephalomyelitis in multiple murine strains. *J. Neuroimmunol.* 150: 59–69.
67. Wotjak, C. T. 2003. C57BLack/BOX? The importance of exact mouse strain nomenclature. *Trends Genet.* 19: 183–184.
68. Gu, B. J., W. Zhang, R. A. Worthington, R. Sluyter, P. Dao-Ung, S. Petrou, J. A. Barden, and J. S. Wiley. 2001. A Glu-496 to Ala polymorphism leads to loss of function of the human P2X7 receptor. *J. Biol. Chem.* 276: 11135–11142.
69. Wiley, J. S., L. P. Dao-Ung, C. Li, A. N. Shemon, B. J. Gu, M. L. Smart, S. J. Fuller, J. A. Barden, S. Petrou, and R. Sluyter. 2003. An Ile-568 to Asn polymorphism prevents normal trafficking and function of the human P2X7 receptor. *J. Biol. Chem.* 278: 17108–17113.
70. Denlinger, L. C., K. Schell, G. Angelini, D. Green, A. Guadarrama, U. Prabhu, D. B. Coursin, K. Hogan, and P. J. Bertics. 2004. A novel assay to detect nucleotide receptor P2X7 genetic polymorphisms influencing numerous innate immune functions. *J Endotoxin Res.* 10: 137–142.
71. Denlinger, L. C., G. Angelini, K. Schell, D. N. Green, A. G. Guadarrama, U. Prabhu, D. B. Coursin, P. J. Bertics, and K. Hogan. 2005. Detection of human P2X7 nucleotide receptor polymorphisms by a novel monocyte pore assay predictive of alterations in lipopolysaccharide-induced cytokine production. *J. Immunol.* 174: 4424–4431.
72. Wiley, J. S., L. P. Dao-Ung, B. J. Gu, R. Sluyter, A. N. Shemon, C. Li, J. Taper, J. Gallo, and A. Manoharan. 2002. A loss-of-function polymorphic mutation in the cytolytic P2X7 receptor gene and chronic lymphocytic leukaemia: a molecular study. *Lancet* 359: 1114–1119.
73. Dao-Ung, L. P., S. J. Fuller, R. Sluyter, K. K. SkarRatt, U. Thunberg, G. Tobin, K. Byth, M. Ban, R. Rosenquist, G. J. Stewart, and J. S. Wiley. 2004. Association of the 1513C polymorphism in the P2X7 gene with familial forms of chronic lymphocytic leukaemia. *Br. J. Haematol.* 125: 815–817.
74. Thunberg, U., G. Tobin, A. Johnson, O. Soderberg, L. Padyukov, M. Hultdin, L. Klareskog, G. Enblad, C. Sundstrom, G. Roos, and R. Rosenquist. 2002. Polymorphism in the P2X7 receptor gene and survival in chronic lymphocytic leukaemia. *Lancet* 360: 1935–1939.
75. Adinolfi, E., L. Melchiorri, S. Falzoni, P. Chiozzi, A. Morelli, A. Tieghi, A. Cuneo, G. Castoldi, F. Di Virgilio, and O. R. Baricordi. 2002. P2X7 receptor expression in evolutive and indolent forms of chronic B lymphocytic leukemia. *Blood* 99: 706–708.
76. Di Virgilio, F., and J. S. Wiley. 2002. The P2X7 receptor of CLL lymphocytes-a molecule with a split personality. *Lancet* 360: 1898–1899.